J. Quant. Spectrosc. Radiat. Transfer Vol. 28, No. 3, pp. 223–231, 1982
Printed in Great Britain.

0022-4073/82/090223-09$03.00/0

THE VACUUM ULTRAVIOLET SPECTRA OF HCN, C_2N_2, AND CH_3CN

JOSEPH A. NUTH†

Chemistry Department, University of Maryland, College Park, MD 20740, U.S.A.

and

SOL GLICKER

Astrochemistry Branch, Laboratory for Extraterrestrial Physics, Goddard Space Flight Center, Greenbelt, MD 20771, U.S.A.

(*Received* 21 *October* 1981)

Abstract—Quantitative vacuum ultraviolet absorption spectra for HCN, C_2N_2, and CH_3CN have been obtained over the wavelength range 60 nm $\leq \lambda \leq$ 160 nm. Where comparison is possible, our measurements of the absorption coefficients for HCN and C_2N_2 are consistent with previous studies. Because of the superior resolution of this work (0.05 nm), vibrational assignments in the valence and Rydberg transitions of HCN have been extended while higher members of the Rydberg series in CH_3CN have been identified.

1. INTRODUCTION

HCN and CH_3CN have been identified via radio techniques in both comets[1] and the interstellar medium,[2] while HCN has recently been identified in the atmosphere of Titan.[3] although C_2N_2 has yet to be observed, the abundance of CN reported in such studies, coupled with the difficulty of its detection via radio techniques, argues strongly for its presence. All three molecules can be important starting materials in chemical reactions leading to the formation of the highly complex species observed in the interstellar medium and could also play key roles in the chemical evolution of life on earth.

In order to calculate the lifetime of molecules in the interstellar medium, quantitative spectra in the vacuum ultraviolet are essential.[4] This information is also necessary to calculate theoretically the rate of production of the CN radical in comets. Three of the most likely parent molecules of CN are HCN, C_2N_2, and CH_3CN. Finally, as astronomers begin to look into the far u.v.,[5] quantitative spectra of molecules such as C_2N_2, which are extremely difficult to detect by standard radio techniques, might be the only means by which these molecules are observed.

Presently, only one quantitative study of the absorption of C_2N_2 has been published and this was done at a resolution of only 0.1 nm.[6] Similarly, one quantitative study of the absorption spectrum of HCN has been published at 0.08 nm resolution[7] and another is available from West.[8] A third study, which compares the spectra of HCN and DCN in the wavelength range 130–80 nm at 0.3 nm resolution, will soon be available.[24] No quantitative spectra are available for CH_3CN. Other available studies of these molecules have either relied on early photographic work or on electron impact energy loss spectrometry. We have therefore measured the absorption coefficients of HCN, C_2N_2, and CH_3CN from 60 to 160 nm at 0.05 nm resolution. We have compared our results with previous work wherever possible.

2. EXPERIMENTAL

(a) *Apparatus*

Figure 1 shows a schematic diagram of the apparatus used in obtaining total absorption coefficients in the 60–168 nm wavelength region. The apparatus has been described elsewhere by Gentieu and Mentall;[9] however, some additional details are given here. The position of the double beam mirror and other items shown in Fig. 1 were controlled by an IBM 1800 computer. The system was windowless and a steady gas flow was maintained with a standard leak valve. The gas pressures were measured with a calibrated Baratron type 170M capacitance manometer.

A McPherson Model 225, 1-m normal incidence monochromator was fitted with differentially pumped entrance slits, a McPherson Model 665 double beam attachment, and a

†Present address: NAS/NRC Resident & Research Associate, Code 691, Goddard Space Flight Center, Greenbelt, MD 20771, U.S.A.

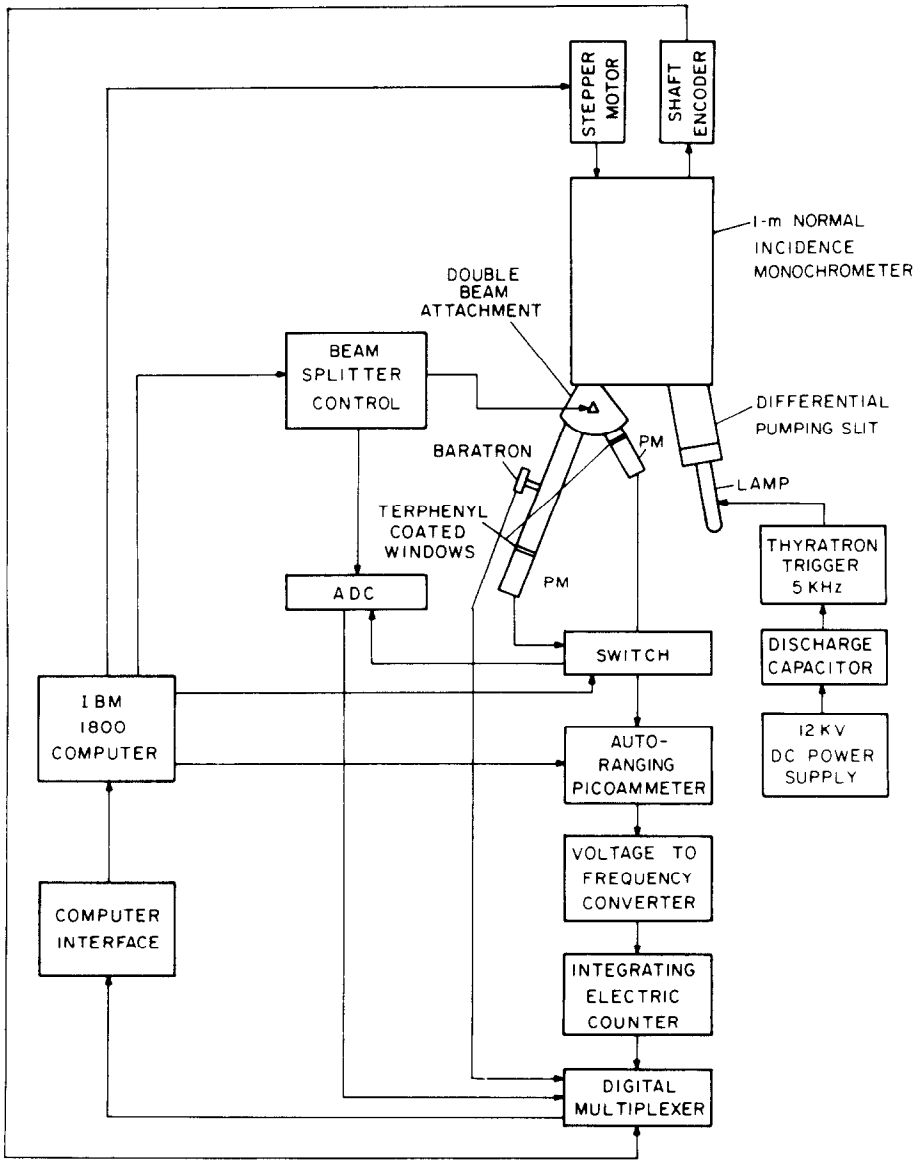

Fig. 1. Schematic diagram of the apparatus used to measure absorption coefficients.

1200 line/mm concave diffraction grating. The sample beam port of the double beam attachment contained a stainless steel sample cell (42.5 cm in length) followed by a terphenyl coated window and an EMI 9635A photomultiplier. The reference beam port of the double-beam attachment was fitted with a second matched terphenyl coated window and an EMI 9635A photomultiplier. A resolution of 0.05 nm (i.e., full width at half maximum) was maintained over the entire wavelength range using 50 μm fixed slits.

The signals from the alternately switched sample and reference photomultipliers were fed to an autoranging picoammeter and then to instrumentation (Fig. 1) used to complete the analog voltage measurement. An integration time of 30 sec provided a 1% reproducibility for the sample to reference beam ratio and an overall estimated error of 5%. The resultant absorption coefficients were provided by an IBM 1627 plotter for sample pressures of 10–125 mtorr, depending upon the value of the coefficients. Pressure effects on selected peaks were absent in the pressure range accessible (ca. 2 fold).

(b) *Light sources and sample gases*

Four lamps were used to cover the wavelength region. A Hopfield continuum lamp[10] provided a continuum source in the 60 to approx. 105 nm region. Three microwave excited

continuum lamps[11] containing 250 torr of Ar, Kr, and Xe, respectively, were used to cover the remainder of the wavelength region reported in this work. The Ar lamp was fitted with a lithium fluoride window, while the Kr and Xe lamps contained magnesium fluoride windows. A Raytheon Model PGM-10 microwave generator rated at 85 watts and 2450 mhz was used to operate the Ar, Kr, and Xe lamps.

Reagent grade methyl cyanide and cyanogen (99% purity) were obtained from the J. T. Baker and the Matheson Co., respectively. Hydrogen cyanide was generated from a KCN and stearic acid mixture heated under vacuum to approximately 100°C. The materials were purified under vacuum by bulb-to-bulb distillation. The gases were stored in 2 l. glass bulbs and attached to the flow system as needed. Mass spectral analysis of the three gases indicated only H_2O and CO_2 impurities (0.1% maximum).

3. RESULTS

Figures 2–4 give the total absorption coefficients obtained in this work for HCN, C_2N_2 and CH_3CN, respectively. The total absorption coefficients were calculated from Lambert's law,

$$k = L^{-1}(760/P)(T/273)\ln(I_0/I), \tag{1}$$

where k is given in cm^{-1} at STP, with L, P, T, I_0, and I, representing the experimental path length (cm), pressure (torr), experimental temperature (°K), incident intensity, and transmitted intensity, respectively.

From Fig. 1, one observes a difference in path length between the sample beam and the reference beam equal to the length of the sample cell. A typical value of 1.5 was obtained for the ratio of the reference to sample beam intensity in the absence of a sample gas. The large value of the signal ratio was caused by the divergent beam formed at the double-beam mirror. Exchanging terphenyl windows and/or photomultipliers produced no change in the relative signals. In addition, it was found that the previous history of the terphenyl phosphor affected the ratio. Consequently, prior to each measurement, the entire system was exposed to the sample gas, then evacuated and a background recorded (i.e., sample/reference signal) over the wavelength region of interest. The transmission (I/I_0) used in (Ref. 1) was the relative signal obtained in the presence of sample gas divided by the background ratio. A second background scan was made at the completion of each sample scan, since in a few runs a measurable

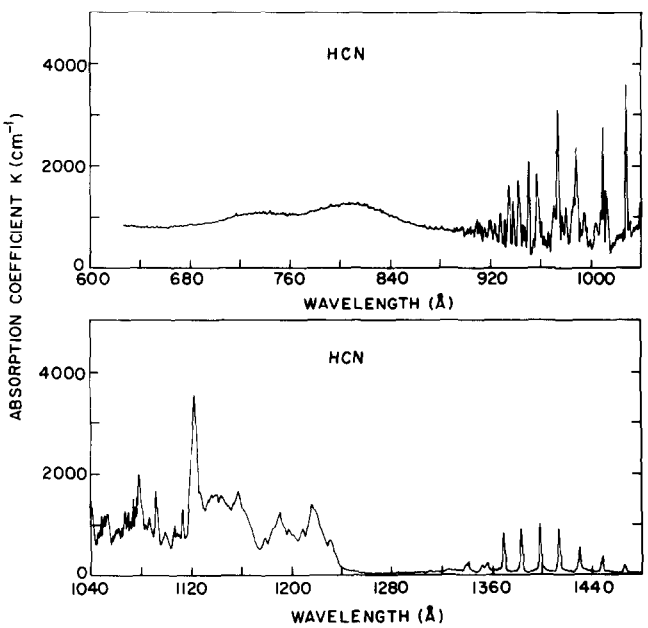

Fig. 2. Total absorption coefficients (k cm^{-1} atm^{-1}) of HCN vs incident photon wavelength (nm).

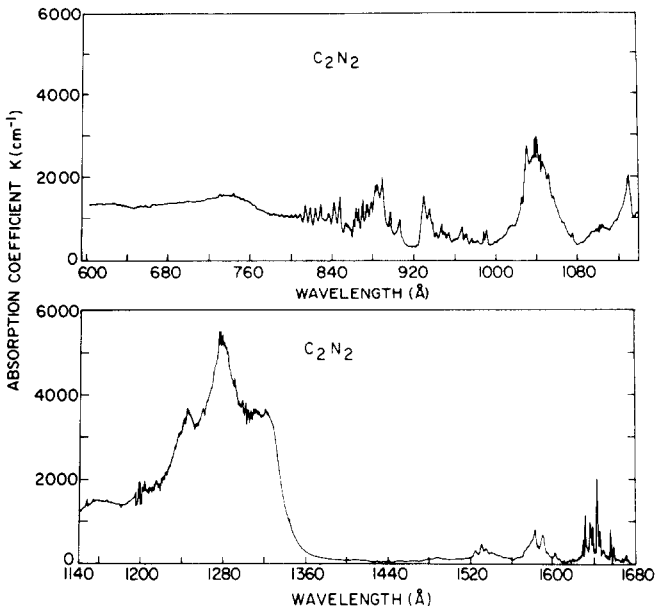

Fig. 3. Total absorption coefficients (k cm^{-1} atm^{-1}) of C_2N_2 vs incident photon wavelength (nm).

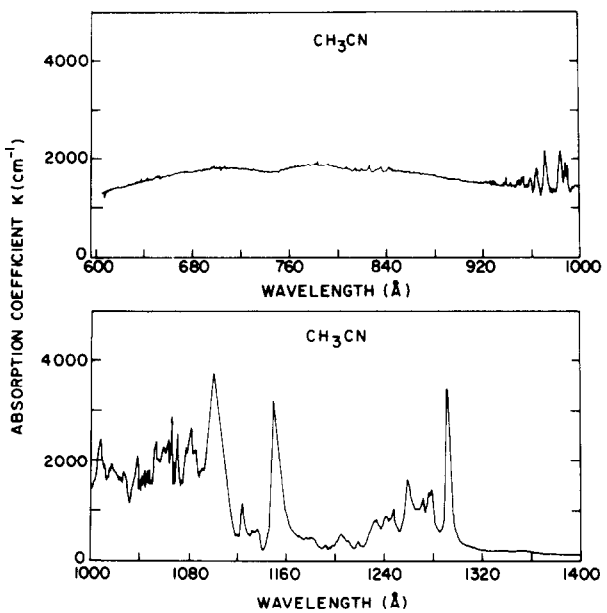

Fig. 4. Total absorption coefficients (k cm^{-1} atm^{-1}) of CH_3CN vs incident photon wavelength (nm).

difference between the two were found. An average of the two backgrounds introduced an error of only 1% in the absorption coefficients.

4. DISCUSSION

(a) *Hydrogen cyanide*

The spectrum of HCN between 62 and 148 nm appears in Fig. 2. An ionization continuum is shown containing a weak vibrational structure that continues to the first adiabatic ionization potential at 89.1 nm (Table 1). A complex set of Rydberg series, starting at about 122 nm, appears to converge to the first ionization potential (Table 2). The series which converges to the second ionization potential overlaps this first series[12] and begins at about 116 nm (Table 2). We assign the remaining peaks between 105 and 112 nm to the $^1\Pi \leftarrow \tilde{X}$ transition, in agreement with

Table 1. Ionization potentials and CN($B^1\Sigma$) threshold energies.

Material	Adiabatic IP (eV), from Ref. 14	Threshold Energy (eV)
HCN	13.60 (91.2 nm)	8.40 (147.6 nm), Ref. 17
C_2N_2	13.36 (92.8 nm)	8.82 (140.6 nm), Ref. 17
	14.49 (85.6 nm)	
	14.86 (83.4 nm)	
	15.47 (80.1 nm)	
CH_3CN	12.21 (101.5 nm)	8.52 (145.5 nm), Ref. 23
	13.14 (94.4 nm)	
	(13.13), Ref. 19	

the work of Fridh and Asbrink[13] (Table 3). The $\tilde{D} \leftarrow \tilde{X}$ transition between 128 and 140 nm as well as the $\tilde{C} \leftarrow \tilde{X}$ transition between 130 and 147 nm is also observed (Table 3). In each case where comparison is possible with the work of Fridh and Asbrink[13] or that of Lee[7], our agreement is easily within the limits of error quoted by the aforementioned authors in both peak position[7,13] and absorption coefficient.[7]

(b) *Cyanogen*

The spectrum of C_2N_2 between 60 and 168 nm is shown in Fig. 3. The region between 60 and 80 nm is dominated by a broad ionization continuum upon which a very weak vibrational structure has been superimposed. Between 80 and 105 nm, there appear to be at least four overlapping Rydberg series which converge to adiabatic ionization potentials obtained from photoelectron spectroscopy and indicated in Table 1. It should be noted that Price and Walsh[15] in their early photographic studies indicated the presence of only one series converging around 85–90 nm, while Bell *et al.*[16] in a later photographic study indicated two such series.

Between 125 and 132 nm, we observe a diffuse system identified by Price and Walsh[15] as due to the $\tilde{C} \leftarrow \tilde{X}$ transition. These same authors also assigned the complex vibrational features between 145 and 170 nm to the $\tilde{B} \leftarrow \tilde{X}$ transition. Connors, Roebber and Weiss[6] made a photoelectric study of the region between 105 and 170 nm as a function of total pressure in order to identify Rydberg transitions in C_2N_2. They concluded that all observed transitions in this region were intervalent and suggested that the diffuse band seen between 107 and 132 nm is composed of two or more electronic transitions. The long wavelength end of the latter transitions corresponds to the appearance of CN($B^2\Sigma^+$), as determined by Davis and Okabe[17] at 140.5 nm (Table 1). Scans at higher pressures (this work) in the 140.5 nm region (not shown) indicate that the threshold for the production of the CN ($B^2\Sigma^+$) radical corresponds closely to the onset of the broad continuum in this region.

It is difficult to compare the quantitative results of Conors, Roebber and Weiss[6] with those

Table 2. Rydberg series in HCN.

Vibrational Level	n = 3		n = 4		n = 5		n = 6		n = 7		n = 8	
	λ[a]	k[b]	λ	k	λ	k	λ	k	λ	k	λ	k
First ionization potential as limit ($\tilde{X}^2\Pi$)												
$1\Pi \rightarrow ns\sigma$ (→ 13.607 eV)												
000	1216.3	1396.1	1027.9	3607.9	973.4	3134.9	950.2	2082.9	937.8	1321.5	930.7	994.1
020	1201.6	783.3	1017.4	508.8	966.3	739.5						
001	1190.6	1243.7	1009.3	2796.5	956.8	1837.5	934.5	1631.5				
100			995.1	1098.3	947.2	789.3	922.7	887.9				
002	1163.5	1208.3										
$1\Pi \rightarrow nd\sigma$ (→ 13.607 eV)												
000	1075.7	1305.7	988.5	2383.8	957.4	1491.6	945.4	840.4				
001	1053.0	1208.5	970.4	1222.9	942.6	1250.7	927.7	899.4				
100	1040.0	1356.1										
002	1037.2	854.8										
Second ionization potential as limit ($\tilde{A}^2\Sigma^+$)												
$5\sigma \rightarrow ns\sigma$ (→ 14.011 eV)												
00^0_0	1158.1	1647.3	988.5	2383.8	942.0	1708.3	919.5	1000.7	908.8	1002.9		
02^0_0	1145.7	1560.2	979.8	1220.9	933.5	719.6	911.0	941.9	901.2	821.5		
00^0_1	1136.7	1611.7										
10^0_0	1112.8	1328.4										
10^0_1	1092.0	1646.3										
$5\sigma \rightarrow np\sigma$ (→ 14.011 eV)												
00^0_0	1078.7	1975.1	968.9	902.3								
02^0_0	1067.3	1217.8	960.4	936.5								
00^0_1	1054.6	1048.3										
10^0_0	1048.2	1200.5										
$5\sigma \rightarrow nd\sigma$ (→ 14.011 eV)												
00^0_0	1040.8	1466.2	958.2	1268.9	927.1	1124.8						

a. all wavelengths in Angstroms

b. absorption coefficients in units of cm^{-1} at STP

Table 3. Valence transitions in HCN.

	v'	λ	k	$\nu_2'(cm^{-1})$	$\Delta\nu_2'(cm^{-1})$	λ^a	λ^b
$1\pi \rightarrow \pi^*$	030	1465.9	170.5	68217	863	1465.7	1465.6
	040	1447.6	362.6	69080	845	1447.5	1447.6
$\tilde{C}^1A'$	050	1429.9	522.8	69935	811	1429.8	1430.1
	060	1413.5	904.3	70746	769	1413.5	1413.7
	070	1398.3	1015.2	71515	781	1398.3	1397.7
	080	1383.2	884.9	72296	750	1383.3	1383.0
	090	1369.0	828.3	73046	695	1369.1	
	0100	1356.1	246.1	73741	825	1356.0	1355.8
	0110	1341.1	265.6	74566	872	1341.3	
	0120	1325.6	90.9	75438	782	1325.7	1330.0
	0130	1312.0	80.0	76220	703	1312.1	
	0140	1300.0	40.8	76938			

	v'	λ	k	$\nu'(cm^{-1})$	$\Delta\nu_1$	$\Delta\nu_3$	λ^b
$1\pi \rightarrow \pi^*$	00^0_0	1396.7	99.5	71597			1396.1
	00^0_1	1365.7	134.4	73223		1626	1367.7
$\tilde{D}^1A'$	10^0_0	1352.0	197.9	73964	2367		1351.3
	00^0_2	1338.7	184.5	74699		1476	1340.4
	10^0_1	1325.2	91.6	75460		(1496)	1324.6
	00^0_3	1311.6	79.8	76243		1544	1312.7
	20^0_0	1309.8	70.8	76348	2384		
	10^0_2	1302.4	50.0	76781		(1321)	1303.1
	00^0_4	1285.3	42.4	77803		1560	1286.2
	10^0_3	1279.5	30.9	78156		(1375)	

	v'	λ	k	$\nu'(cm^{-1})$	$\Delta\nu_1$	$\Delta\nu_2$	$\Delta\nu_3$	λ^b
$5\sigma \rightarrow \pi^*$	00^0_0	1122.8	3540.9	89063				1123.5
	01^0_0	1114.6	747.3	89718		655		
$^1\Pi$	02^0_0	1106.2	1001.3	90400		682		1107.8
	00^0_1	1099.0	845.8	90992			1929	1099.6
	01^0_1	1091.0	956.8	91659		(667)		
	10^0_0	1086.5	1167.9	92039	2976			1086.5
	02^0_1	1082.3	1062.6	92396		(737)		
	11^0_0	1079.3	1862.0	92653		(614)		
	00^0_2	1075.7	1305.7	92963			1971	
	03^0_1	1074.1	1511.9	93101		(705)		
	12^0_0	1070.7	1076.9	93396		(743)		
	13^0_0	1061.9	965.2	94171		(775)		
	20^0_0	1052.0	1088.2	95057	3018			

a. from reference 7
b. from reference 13

of this work because the former measurements were made at a resolution of 0.1 nm while those of this work were made at 0.05 nm. It is well known that the true molecular absorption coefficient is obtained only when the monochromator bandwidth is much less than the actual bandwidth of the molecular absorption.[18] For $\lambda < 135$ nm, the molecular bands are broad and the measured coefficients should therefore correspond to the absolute coefficients[7] (see Fig. 3). This will most likely not be the case in the region near 164 nm since very sharp features are observed. In general, our results are consistent with those of Connors *et al.*[6] when one accounts for the higher resolution of our work. Therefore, in the highly structured region near 164 nm, our peaks are higher and valleys lower than their measurements while, in the more diffuse regions, our measurements are within experimental error.

(c) *Methyl cyanide*

The spectrum of CH_3CN between 60 and 140 nm appears in Fig. 4. The region between 60 and 94 nm is dominated by a broad ionization continuum upon which is superimposed a weak vibrational structure. Fridh[19] has assigned the diffuse structure around 107 nm to the $2e \rightarrow 3e\,^1\Sigma^+$ valence transition and predicts that the $1e \rightarrow 3e\,^1\Sigma^+$ transition should have an energy of 12.4 eV.

Table 4. Rydberg series in CH_3CN.

Vibrational Level (ν_2, ν_3, ν_4)	n = 3		n = 4		n = 5		n = 6		n = 7		n = 8		n = 9	
	λ[a]	k[b]	λ	k	λ	k	λ	k	λ	k	λ	k	λ	k
First Ionization Potential as Limit														
$2e \rightarrow np\sigma$ (→ 12.21 eV)														
000	1292.2	3430	1135.6	663	1081.4	2672	1058.2	2168	1046.4	1811	1037.4[d]	2081	1032.3	1156
001	1278.9	1453	1124.4	1158	1070.9	2549	1049.0	1622	1035.4[c]	1581				
100	1259.8	1671	1109.3	2077	1059.6	2286	1037.4[d]	2081	1023.7	1649				
101	1248.0	1062	1100.5	3724	1050.6	1658	1027.7	1791	1015.9	1819				
200	1232.9	896	1090.1	1823	1039.6	1959	1017.1	1939	1005.3	1669				
201	1217.8	403	1079.0	2245	1030.1	1485	1007.7	2368	996.1	1442				
$2e \rightarrow np\pi$ (→ 12.21 eV)														
000	1281.1	909	1126.4	745	1077.0	2258	1055.6	2058	1044.0	1852			1031.9	1152
100	1242.0	927	1096.5	2875	1050.0	1574	1030.5	1299	1018.9	1873				
$2e \rightarrow nd\sigma$ (→ 12.21 eV)														
000	1204.7	547	1104.9	3051	1069.8	2038	1052.0	2270	1041.6	1667				
100	1180.7	496	1086.1	2240	1051.0	1717	1033.9	1479	1023.1	1656				
$2e \rightarrow ns\sigma$ (→ 12.21 eV)														
000	1388.4	373	1154.0	2143	1092.9	1856	1062.8	2326	1048.2	1843	1038.8	2130	1033.5	1438
Second Ionization Potential as Limit														
$7a_1 \rightarrow np\sigma$ (→ 13.13 eV)														
000	1276.1	1380	1068.2	2218	1008.3	2420	984.2	2150	972.0	2168	964.4	1814	960.2	1589
010			1053.8	2414	994.9	1399	971.4	2083	959.4	1601	952.1	1618	947.7	1480
$7a_1 \rightarrow np\pi$ (→ 13.13 eV)														
000	1150.4	3202	1038.4	2161	996.7	1472	978.8	1382	968.2	1260	962.4	1382	958.3	1557
010	1133.2	623	1024.1	1683	982.4	1659	965.2	1597	956.5	1464	950.1	1560	946.5	1439
$7a_1 \rightarrow nd\sigma$ (→ 13.13 eV)														
000	1091.3	1882	1018.3	1899	989.8	1886	976.2	1423	965.8	1618	960.8[c]	1443	957.1	1410

a. all wavelengths in units of Angstroms
b. absorption coefficients in units of cm^{-1} at STP
c. shoulder
d. overlapping peaks

This may correspond to the diffuse structure near 102 nm seen in Fig. 4. Analysis of the valence transitions in CH_3CN is complicated by the fact that the spectrum is dominated by Rydberg transitions (Table 4) converging to both the first and second ionization potentials at 12.21 eV and 13.13 eV respectively (Table 1). Our analysis of these transitions both confirm and extend those of Fridh.[19]

Our spectrum is consistent with the early photographic work of Cutler[20] and of Herzberg and Scheibe[21] but does not show the broad structure near 95 nm observed by Stradling and Loudon.[22] Since Fridh[19] also failed to observe this feature, we suspect that his interpretation is correct and that the feature is due to a N_2 impurity.

CONCLUSION

Quantitative absorption spectra for HCN, C_2H_2, and CH_3CN have been obtained at 0.05 nm resolution from 60 to approx. 160 nm. Data points were recorded every 0.02 nm and transferred to punched cards. These data are available upon request from the authors.

Acknowledgements—We would like to thank E. P. Gentieu and J. E. Mentall for the use of their excellent spectroscopic equipment and for a number of valuable suggestions. We would also like to thank L. J. Stief, R. Cody, and B. Donn for their help and encouragement.

REFERENCES

1. (a) L. E. Snyder and D. Buhl, *Astrophys. J.* **163**, L47 (1971). (b) W. F. Huebner, L. E. Snyder, and D. Buhl, *Icarus* **23**, 580 (1974).
2. (a) P. M. Solomon, K. B. Jefferts, A. A. Penzias, and R. W. Wilson, *Astrophys. J.* **168**, L107 (1971). (b) B. L. Ulich and E. K. Conkling, *Nature* **248**, 121 (1974).
3. R. Hanel *et al.*, *Science* **212**, 192 (1981).
4. L. J. Stief, B. Donn, S. Glicker, E. P. Gentieu, and J. E. Mentall, *Astrophys. J.* **171**, 21 (1972).
5. J. E. Holberg *et al.*, *Astrophys. J.* **242**, L119 (1980).
6. R. E. Connors, J. L. Roebber, and K. Weiss, *J. Chem. Phys.* **60**, 5011 (1974).
7. L. C. Lee, *J. Chem. Phys.* **72**, 6414 (1980).
8. G. A. West, Ph.D. Thesis, University of Wisconsin, Madison (1975).
9. E. P. Gentieu and J. E. Mentall, *J. Chem. Phys.* **64**, 1376 (1976).
10. R. E. Huffman, J. C. Larabee, and D. Chambers, *Appl. Opt.* **4**, 1145 (1965).
11. J. A. R. Samson, *Techniques of Vacuum Ultraviolet Spectroscopy*. Wiley, New York (1967).
12. D. C. Frost, S. T. Lee, and C. A. McDowell, *Chem. Phys. Lett.* **23**, 472 (1973).
13. C. Fridh and L. Asbrink, *J. Elec. Spectrosc. Rel. Phen.* **7**, 119 (1975).
14. D. W. Turner, C. Baker, A. D. Baker, and C. R. Brundle, *Molecular Photoelectron Spectroscopy*, p. 345f. Wiley, New York (1970).
15. W.C. Price and A. D. Walsh, *Trans. Faraday Soc.* **41**, 381 (1945).
16. S. Bell *et al.*, *J. Molec. Spectrosc.* **39** 162 (1969).
17. D. D. Davis and H. Okabe, *J. Chem. Phys.* **49**, 5526 (1968).
18. R. D. Hudson, *Rev. Geophys. Space Phys.* **9**, 305 (1971).
19. C. Fridh, *J. C. S. Faraday Trans. II* **74**, 2193 (1978).
20. J. A. Cutler, *J. Chem. Phys.* **16**, 136 (1948).
21. G. Herzberg and G. Scheibe, *Zeits. f. Phy. Chem.* **B7**, 390 (1930).
22. R. S. Stradling and A. G. Loudon, *J. C. S. Faraday Trans. II* **73**, 623 (1977).
23. H. Okabe and J. Dibeler, *Chem. Phys.* **59**, 2430 (1973).
24. T. Nagata, T. Kondow, Y. Ozaki, and K. Kuchitsu, *Chem. Phys.* **57**, 45 (1981).